Journal of Nuclear Medicine, published on August 2, 2018 as doi:10.2967/jnumed.118.215913

FAPI-PET/CT: biodistribution and preliminary dosimetry estimate of two DOTA-containing FAP-targeting agents in patients with various cancers

Frederik L. Giesel[1*], Clemens Kratochwil[1*], Thomas Lindner[1], Manfred-M. Marschalek[1], Anastasia Loktev[1], Wencke Lehnert[3], Jürgen Debus[4,5], Dirk Jäger[6], Paul Flechsig[1], Annette Altmann[1], Walter Mier[1], Uwe Haberkorn[1,2,7§]

(1) Department of Nuclear Medicine, University Hospital Heidelberg, Heidelberg Germany.
(2) Clinical Cooperation Unit Nuclear Medicine, German Cancer Research Center (DKFZ), Heidelberg, Germany.
(3) ABX-CRO advanced pharmaceutical services Forschungsgesellschaft m.b.H, Dresden, Germany
(4) Dept. of Radiation Oncology, University Hospital Heidelberg, Heidelberg, Germany
(5) Clinical Cooperation Unit Radiation Oncology, German Cancer Research Center (DKFZ), Heidelberg, Germany
(6) Dept. of Medical Oncology, National Center for Tumor Diseases (NCT), Heidelberg, Germany
(7) Translational Lung Research Center Heidelberg (TLRC), German Center for Lung Research (DZL), Heidelberg, Germany

*Authors contributed equally.

Conflicts of interest: Patent application for quinoline based FAP-targeting agents for imaging and therapy in nuclear medicine (UH, AL, TL, *WM*).

§ Corresponding author:

Uwe Haberkorn
Department of Nuclear Medicine, University Hospital Heidelberg
Im Neuenheimer Feld 400, 69120 Heidelberg
Tel: +49-6221-56-7731
Fax: +49-6221-56-5288

Immediate Open Access: Creative Commons Attribution 4.0 International License (CC BY) allows users to share and adapt with attribution, excluding materials credited to previous publications.
License: https://creativecommons.org/licenses/by/4.0/.
Details: http://jnm.snmjournals.org/site/misc/permission.xhtml.

Abstract

Purpose: Fibroblast activation protein (FAP) is overexpressed in cancer associated fibroblasts of several tumor entities. Recent development of quinoline based positron-emission-tomography (PET)-tracers that act as FAP-Inhibitors (FAPI) demonstrated promising results preclinically and already also in few clinical cases. Consecutively this novel tracer is now applied in our hospital to amend the diagnostics of cancer patients facing limitations of standard exams. Here we analyze the tissue biodistribution and preliminary dosimetry of two members of this new class of PET-radiopharmaceuticals.

Methods: A preliminary dosimetry estimate for FAPI-02 and FAPI-04 was based on two patients examined at 0.2h, 1h and 3h after tracer injection using the QDOSE dosimetry software suit. Further PET/CT scans of tumor patients were acquired 1 h after injection of either FAPI-02 (n=25) or FAPI-04 (n=25); for 6 patients an intra-individual related FDG-scan (also acquired 1h p.i.) was available. For the normal tissue of 16 organs, a 2 cm Spheric-VOI was placed in the parenchyma, for tumor lesions a threshold segmented VOI was used to quantify $SUV_{mean/max}$.

Results: Very similar to literature values for ^{18}F-FDG, ^{68}Ga-DOTATATE or ^{68}Ga-PSMA-11, an exam with 200 MBq ^{68}Ga-FAPI-2/4 corresponds to an equivalent dose of approx. 3-4 mSv. After a fast clearance via the kidneys the normal organs showed a low tracer uptake with only minimal changes between 10 min and 3 h p.i.. In FAPI-02 the tumor uptake from 1h to 3h p.i. decreased by 75%, whereas the tumor retention was prolonged with FAPI-04 (25% washout). Regarding tumor-to-background ratios, at 1h p.i. both FAPI-tracers performed equally. In comparison to FDG the tumor uptake was almost equal (average SUV_{max}-FDG 7.41; SUV_{max}-FAPI-2 7.37; n.s.); the background uptake in brain (11.01 vs 0.32), liver (2.77 vs 1.69) and oral/pharyngeal mucosa (4.88 vs 2.57) was significantly lower with FAPI; other organs were not relevantly different between FDG and FAPI.

Conclusion: FAPI-PET/CT is a new diagnostic method in imaging cancer patients. In contrast to FDG no diet/fasting in preparation of the exam is necessary and image acquisition can potentially be started few minutes after tracer application. Tumor-to-background contrast ratios were equal or even improved in comparison to FDG.

Introduction

Fibroblast activation protein (FAP) is highly expressed in the stroma of several tumor entities. Especially breast, colon and pancreatic carcinomas are characterized by a strong desmoplastic reaction, which causes that 90% of the gross tumor-mass can consist from stromal but not tumor cells.

Fibroblasts are present ubiquitary in the whole body and show dipeptidyl peptidase 4 (DPP4) expression, but no or only a very low FAP expression. In contrast, cancer associated fibroblasts (CAFs) are specifically characterized by the expression of FAP, which has in contrast to the closely related DPP4 not only exopeptidase but also endopeptidase activity; i.e. proteins can not only be cleaved at their terminal end but at any post-proline bond in the amino acid sequence (*1*). Thus, CAFs differ from normal fibroblasts by providing FAP as a target with a relatively high tumor-specific expression and FAP specific inhibitors (FAPI) have already been developed as cancer drugs (*2,3*).

Based on a quinoline-based FAP specific inhibitor (*2*), a new class of radiopharmaceuticals was designed and found preclinically highly promising as molecular targeting imaging probes and hopefully also as therapeutically useful (*4,5*). Few first-in-human cases demonstrated high contrast tumor imaging and possible appropriateness as a pan-tumor agent (*4,5*).

Consecutively, we now growingly use this novel tracer to amend the diagnostics of cancer patients which are facing limitations of standard exams.

Here we approximated the radiation exposure of FAPI-PET/CT, based on the ligands FAPI-02 and FAPI-04, with serially performed PET-scans and analyzed the normal tissue biodistribution and tumor uptake of these FAPI-ligands in comparison to the current standard Fluorodesoxyglucose (FDG).

Methods

Patients

All patients gave written informed consent to receive FAPI-PET/CT following the regulations of the German Pharmaceuticals Act §13(2b). All patients were referred to the experimental diagnostics by their caring oncologist, which were facing an unmet diagnostic challenge, which could not be solved sufficiently with standard diagnostic means. For example this could be insufficient tumor delineation for target-volume segmentation before external beam radiotherapy, or lesions that were considered suspicious for FDG "false-negatives", or to select target-positive patients for experimental last-line therapy with therapeutic FAPI-conjugates. The data were analyzed retrospectively with approval of the local ethics committee (No. S016/2018). Detailed patient characteristics are provided in Table-1.

Radiopharmaceuticals

Synthesis and labeling of FAPI-02 (*4*) and FAPI-04 (*5*) has already been described previously. FDG was obtained commercially (FCON, Holzhausen, Germany). The chemical structures of FAPI-02 and FAPI-04 are provided in Figure-1.

PET/CT-imaging

All imaging was performed on a Biograph mCT Flow scanner (Siemens, Erlangen, Germany). Following non-contrast-enhanced low-dose CT (130keV, 30mAs, CareDose; reconstructed with a soft-tissue kernel to a slice thickness of 5mm), PET was acquired in 3-D mode (matrix 200 × 200) using FlowMotion (Siemens). The emission data was corrected for randoms, scatter and decay. Reconstruction was performed with an ordered subset expectation maximization (OSEM) algorithm with 2 iterations / 21 subsets and Gauss-filtered to a transaxial resolution of 5 mm at full-width at half-maximum (FWHM); Attenuation correction was performed using the non-enhanced low-dose CT data. The injected activity for

the FAPI exams ranged 122-336 MBq (details provided in Table-1) and the PET scans were started 1h post injection.

To approximate the dosimetry, two patients were imaged 10min, 1h and 3h after injection of 306 MBq FAPI-02 or 258 MBq FAPI-04, respectively.

Adverse events

Standard vital parameters were checked between tracer application and up to 30min after finishing the examination by a medical technician and the patients were asked to self-report any abnormalities.

Radiation dosimetry estimate

The dosimetry analysis was performed using the QDOSE dosimetry software suite (ABX-CRO; Dresden, Germany). Kidneys, liver, spleen, urinary bladder content, red marrow, heart contents and remainder body were included as source organs. As blood sampling failed due to poor vein conditions, the red marrow dose was approximated with the activity segmented with volume-of-interest technic in the PET-scans. The respective non-tumor-affected lumbar vertebra 5 (FAPI-2) and 4 (FAPI-4). were assumed to contain 2.46% of the total red-marrow (*6*). Using QDOSE, all CT images were coregistered using an automatic deformable coregistration. PET images were coupled to the CT of the corresponding imaging session. The PET images were transformed according to the transformation matrix of the coupled CT. The volumes of interest (VOIs) of all segmented source organs were drawn in the respective exam with best organ delineation and then copied onto all other time points to calculate the time activity curves (TACs). Mono-exponential curve fitting was then applied to all organ TACs. The cumulative activity Ã between time 0 and the first measured time point was calculated assuming a linear increase from 0 to the first measured activity. The Ã between the first measured time point and the last measured time point was integrated numerically using trapezoidal approximation. The Ã from the last measured time point to infinity was integrated using the fitted function. The total body Ã was calculated based on the injected activity assuming and the calculated effective half-life in a total body VOI. This approach was chosen as parts of

the body were not in the field of view of the PET/CT. The Ã values of total body and red marrow were added as additional organs into QDOSE. The Ã of the remainder body was then automatically calculated by subtracting all source organs Ã from the total body Ã. All source organ residence times were calculated by dividing the Ã with the injected activity. Absorbed and effective dose calculations were performed using the ICRP endorsed IDAC-Dose 2.1 and IDAC-Dose 1.0 (*7*) which are integrated in QDOSE. In addition, residence times of all included source organs and remainder body were exported as an OLINDA case file for dose calculation in OLINDA 1.1 (*8*). Both, IDAC-Dose 1.0 and OLINDA 1.1, are based on the Cristy-Eckerman stylized phantom series (*9*). IDAC-Dose 2.1 is based on the ICRP Adult Reference Computational Phantoms (*10*) and ICRP Specific Absorbed Fractions (*11*). Organ masses were not adapted to individual subject organ masses.

Biodistribution

The tracer biodistribution in patients was quantified by SUVmean and SUVmax at 1 h post injection for FAPI-02, FAPI-04 and FDG, respectively. The interval between FDG and FAPI exams was nine days maximum and no treatment change was done in between. For calculation of the standardized uptake value (SUV), circular regions of interest were drawn around the tumor lesions with focally increased uptake in transaxial slices and automatically adapted to a three-dimensional VOI with e.soft software (Siemens) at a 40 % isocontour. The normal organs were evaluated with a 1 cm diameter (for the small organs thyroid, parotid gland, myocardium, oral mucosa, spinal cord) to 2 cm diameter (brain, muscle, liver, spleen, kidney, fat, aortic lumen content, lung) sphere placed inside the organ parenchyma.

Results

Adverse events

All patients tolerated the examination well. No drug-related pharmacological effects or physiologic responses occurred. All observed parameters (e.g., blood pressure, heart rate, body temperature) remained normal and unchanged during injection and 1.5h of follow-up. No patient reported any symptoms.

Dosimetry estimate

Maximum intensity projections of the PET-scans used for source organs segmentation are demonstrated in Figure-2. The approximated dosimetry for the two patients is presented in Table-2. The effective dose of FAPI-02 was 1.80E-02 mSv/MBq calculated with OLINDA (1.82E-02 with IDAC1 / ICRP60, 1.79E-02 with IDAC2 / ICRP103). The effective dose for FAPI-04 PET/CT was 1.64E-02 mSv/MBq calculated with OLINDA (1.66E-02 with IDAC1 / ICRP60, 1.35E-02 with IDAC2 / ICRP103). If the delayed scan at 3h p.i. is omitted in clinical practice, the routine activity for an FAPI-exam could be reduced to 200 MBq ^{68}Ga; consecutively the radiation dose of such a FAPI-PET/CT scan would be 3-4 mSv.

Biodistribution

The two patients examined 10 min to 3h p.i. demonstrated that both FAPI-tracers rapidly reach their stable physiological biodistribution. In normal tissue changes between 10 min and 3 h p.i. are minimal over time. Tumor uptake declines by mean 75 % from 1h to 3 h p.i. using FAPI-02; fewer washout of only 25% (mean) between 1h and 3h p.i. (i.e. longer tumor retention) was observed with FAPI-04 (Figure-2, bottom). However, at 1h p.i. (the time point also chosen for comparison to FDG) both FAPI-tracers perform equally in regard to tumor-to-background ratios.

The quantitative tumor uptake of FAPI-PET was very similar in comparison to the current Onco-PET standard-of-reference, the tracer FDG (average SUVmax-FDG 7.41; average SUVmax-FAPI-2 7.37; n.s.). In pancreatic, esophageal, lung, head and neck as well as colorectal cancer the quantitative tumor-uptake was non-inferior in comparison to FDG. In contrast, dedifferentiated thyroid cancer with flip-flop uptake of FDG was not accumulating FAPI (Fig-3). Regarding background activity, the average SUVmax of FAPI-02

was significantly lower in brain (0.32 vs 11.01), liver (1.69 vs 2.77) and oral/pharyngeal mucosa (2.57 vs 4.88). This improved the contrast-ratios for liver metastases of pancreatic and colorectal cancer and delineation of the esophageal cancer (Fig-3). For all other organs FAPI-02 presents no significant difference in comparison to FDG (Fig-4).

Comparing the tumor uptakes of FAPI-02 vs FAPI-04, the average SUVmax presented no relevant differences (FAPI-2 8.37; FAPI-4 10.07; n.s.). Both tracers presented unspecific uptake in location of wound healing after surgical intervention (7.07 vs 6.76; n.s.). Only minor differences between FAPI-02 and FAPI-04 were observed regarding normal organ uptake (Fig-5).

Discussion

Recently cancer associated fibroblasts have been reported as a promising new multi-tumor target for small molecules nuclear diagnostics (*4,5*). In this work we initially approximated the radiation exposure of a FAPI-02 and a FAPI-04 PET, which was found in the dimension of 1.4-1.8 mSv/100MBq, respectively. We further analyzed the normal tissue biodistribution of these FAPI-ligands in comparison to FDG, the current standard in Onco-PET, and found comparable tumor uptakes and, except of a lower brain, liver and oral mucosa uptake of FAPI, also comparable background in normal organs.

The approximated dosimetry is limited by evaluating only one patient per tracer. However, the effective organ half-life and hence the radiation exposure is rather dominated by the short physical half-life of ^{68}Ga (t1/2 68 min) than the biological half-life of the shuttle molecule and thus it was no surprise, that the effective dose of an ^{68}Ga FAPI-02 or FAPI-04 PET (1.4-1.8 mSv/100MBq) is in a similar dimension as with other ^{68}Ga-based tracers such as ^{68}Ga-DOTATOC/DOTATATE (2.1 mSv/100MBq, respectively)(*12*), ^{68}Ga-PSMA-11 (1.6-2.4 mSv/100MBq) (*13,14*) and ^{68}Ga-PSMA-617 (2.1 mSv/100 MBq and also with FDG (2 mSv/100MBq) (*15*) the current standard in Onco-PET.

It was not scope of this work to evaluate the diagnostic accuracy such as sensitivity and specificity of the new modality for a respective tumor entity. However, in a small cohort of challenging patients hampering

various tumor diseases, the quantitative tumor uptake as well as background activity in most normal organs was equal to FDG. A lower uptake in brain, liver and oral-laryngeal mucosa might be promising for evaluation of brain or liver metastases, liver tumors or head-and-neck tumors.

FAPI-PET/CT should also be considered as a complementary tracer for tumor-entities known to poorly perform with FDG, e.g. HCC or pancreatic cancer. Both tumor entities have well known limitations regarding FDG which are not completely covered by specific PET-tracers, yet (*16,17*).

We imaged several tumor entities with comparable tumor-to-background ratios with FAPI and FDG. We found high FAPI uptake in pancreatic cancer, esophageal cancer, NSCLC, head and neck cancer and colon cancer. In contrast, dedifferentiated thyroid cancer showed a low uptake or was FAPI-negative (Fig.-3). In this setting the new imaging probes might benefit from its independency of blood sugar level needing no dietary preparation. The rapid tumor-uptake at 10 min p.i., as demonstrated in Fig.-2, also indicates the possibility of early imaging. This could increase patient comfort due to a shorter waiting and scan time, which can be relevant in sick patients and as a side-aspect the radiation burden of the exam could be reduced if the injected activity can be reduced. Thus, the diagnostic performance of early vs late FAPI-imaging should be evaluated more systematically in future studies. The possibility of early FAPI-imaging would also avoid the 1h uptake time with resting patients, which is considered mandatory for FDG; Consecutively, FAPI-PET could simplify the clinical work-flow.

In contrast to FDG, the FAPI-ligands contain DOTA as chelator which can also be labeled with various therapeutic radionuclides. Taking into account recent successes of radioligand-therapy in neuroendocrine (*18*) and prostate (*19*) cancer, targeting FAP presents also a promising new approach in the treatment of these FAP-positive tumors. However, a further increase of tumor retention time, as in part already achieved in the development step from FAPI-02 to FAPI-04 (Fig.-2) (*5*), would still be required to refine the potential of FAPI-targeting radionuclide therapy.

Similar to FDG, we observed some uptake in post-surgical wound healing because in this condition fibroblasts are also activated. Thus, we would not consider FAPI a more tumor-specific PET-tracer than FDG. However, FDG is rather known to accumulate in acute inflammation, in contrast FAP activation is typical for chronic inflammation already causing fibrotic reaction (*20,21*). Localized FAP activation has also

been reported in other diseases which are followed by tissue remodeling such as myocardial infarction. Thus, FAPI-PET/CT could play a complementary role to FDG in the field of chronic inflammatory cardiac diseases (*22*) or other disease conditions with tissue remodelling.

While the discussed approaches pursued, no final conclusion about their validity can be drawn based on this first proof-of-concept investigation which was intended to evaluate the dosimetry of ^{68}Ga-labeled FAPI-2/4 diagnostics, identifying physiological biodistribution and preliminary target-validation in selected tumor entities. Further studies dedicated to evaluate the diagnostic performance in the respective clinically relevant settings are highly warranted.

Conclusion: FAPI-PET/CT is a promising new diagnostic method for imaging various kinds of cancer, in particular pancreatic, head and neck, colon, lung and breast cancer, with tumor-to-background contrast ratios equal or even improved in comparison to FDG. Favorable characteristics of the new ligands are: a fast tracer kinetics, which seems appropriate to image patients even <1 h after injection; a low background in liver, oral mucosa and brain; and its independence from blood sugar. As the FAPI-tracers contain the universal DOTA-chelator also a theranostic approach - after labeling the ligand with an appropriate therapeutic radionuclide - seems feasible.

References

1. Hamson EJ, Keane FM, Tholen S, Schilling O, Gorrell MD. Understanding fibroblast activation protein (FAP): substrates, activities, expression and targeting for cancer therapy. Proteomics Clin Appl. 2014 Jun;8(5-6):454-63. doi: 10.1002/prca.201300095.
2. Jansen K, Heirbaut L1, Cheng JD2, et al. Selective Inhibitors of Fibroblast Activation Protein (FAP) with a (4-Quinolinoyl)-glycyl-2-cyanopyrrolidine Scaffold. ACS Med Chem Lett. 2013 Mar 18;4(5):491-6. doi: 10.1021/ml300410d.
3. Poplawski SE, Lai JH, Li Y, et al. Identification of selective and potent inhibitors of fibroblast activation protein and prolyl oligopeptidase. J Med Chem. 2013 May 9;56(9):3467-77. doi: 10.1021/jm400351a.
4. Loktev A, Lindner T, Mier W, et al. A new method for tumor imaging by targeting cancer associated fibroblasts. J Nucl Med. 2018 Apr 6. pii: jnumed.118.210435. doi: 10.2967/jnumed.118.210435. [Epub ahead of print]
5. Lindner T, Loktev A, Altmann A, et al. Development of quinoline based theranostic ligands for the targeting of fibroblast activation protein. J Nucl Med. 2018 Apr 6. pii: jnumed.118.210443. doi: 10.2967/jnumed.118.210443. [Epub ahead of print]
6. Hindorf C, Glatting G, Chiesa C, Linden O, Flux G.: EANM Dosimetry Committee guidelines for bone marrow and whole-body dosimetry. Eur J Nucl Med Mol Imaging 37(6): 1238-1250, 2010.
7. Andersson, M., Johansson, L., Eckerman, K., Mattsson, S.: IDAC-Dose 2.1, an internal dosimetry program for diagnostic nuclear medicine based on the ICRP adult reference voxel phantoms. EJNMMI Research 7 (1): 88, 2017.
8. Stabin, M. G., Sparks, R.B., Crowe, E. OLINDA/EXM: the second-generation personal computer software for internal dose assessment in nuclear medicine. J Nucl Med, 46(6):1023-1027, 2005.
9. Cristy, M., Eckerman, K. F.: Specific Absorbed Fractions of Energy at Various Ages from Internal Photon Sources. Oak Ridge: Oak Ridge National Laboratory; ORNL/TM-8381 V1-V7, 1987.
10. Menzel, H. G., Clement, C., DeLuca, P.: ICRP Publication 110. Realistic reference phantoms: an ICRP/ICRU joint effort. A report of adult reference computational phantoms. Ann ICRP, 39(2):1-164, 2009.

11. Bolch, W.E., Jokisch, D., Zankl, M., Eckerman, K.F., Fell, T., Manger, R., Endo, A., Hunt, J., Kim, K.P., Petoussi-Henss, N.: ICRP Publication 133. The ICRP Computational Framework for Internal Dose Assessment for Reference Adults: Specific Absorbed Fractions. Ann ICRP, 45(2), 1–74, 2016.
12. Sandström M, Velikyan I, Garske-Román U, et al. Comparative biodistribution and radiation dosimetry of ^{68}Ga-DOTATOC and ^{68}Ga-DOTATATE in patients with neuroendocrine tumors. J Nucl Med. 2013;54:1755-1759.
13. Pfob CH, Ziegler S, Graner FP, et al. Biodistribution and radiation dosimetry of (68)Ga-PSMA HBED CC-a PSMA specific probe for PET imaging of prostate cancer. Eur J Nucl Med Mol Imaging. 2016;43:1962-1970.
14. Afshar-Oromieh A, Hetzheim H, Kübler W, et al. Radiation dosimetry of (68)Ga-PSMA-11 (HBED-CC) and preliminary evaluation of optimal imaging timing. Eur J Nucl Med Mol Imaging. 2016;43:1611-1620.
15. Johansson L, Mattsson S, Nosslin B, Leide-Svegborn S. Effective dose from radiopharmaceuticals. Eur J Nucl Med. 1992;19:933-938.
16. Yun M, Bang SH, Kim JW, Park JY, Kim KS, Lee JD. The importance of acetyl coenzyme A synthetase for 11C-acetate uptake and cell survival in hepatocellular carcinoma. J Nucl Med. 2009;50:1222-1228.
17. Strobel O, Büchler MW. Pancreatic cancer: FDG-PET is not useful in early pancreatic cancer diagnosis. Nat Rev Gastroenterol Hepatol. 2013;10:203-205.
18. Strosberg J, El-Haddad G, Wolin E, et al. Phase 3 Trial of 177Lu-Dotatate for Midgut Neuroendocrine Tumors. N Engl J Med. 2017 Jan 12;376(2):125-135.
19. Hofman MS, Violet J, Hicks RJ, et al. ^{177}Lu-PSMA-617 radionuclide treatment in patients with metastatic castration-resistant prostate cancer (LuPSMA trial): a single-centre, single-arm, phase 2 study. Lancet Oncol. 2018 May 7. pii: S1470-2045(18)30198-0. doi: 10.1016/S1470-2045(18)30198-0. [Epub ahead of print]
20. Egger C, Cannet C, Gérard C, Suply T, Ksiazek I, Jarman E, Beckmann N. Effects of the fibroblast activation protein inhibitor, PT100, in a murine model of pulmonary fibrosis. Eur J Pharmacol. 2017;809:64-72.

21. Uitte de Willige S, Malfliet JJ, Janssen HL, Leebeek FW, Rijken DC. Increased N-terminal cleavage of alpha-2-antiplasmin in patients with liver cirrhosis. J Thromb Haemost. 2013;11:2029-2036.
22. Tillmanns J, Hoffmann D, Habbaba Y, Schmitto JD, Sedding D, Fraccarollo D, Galuppo P, Bauersachs J. Fibroblast activation protein alpha expression identifies activated fibroblasts after myocardial infarction. J Mol Cell Cardiol. 2015;87:194-203.

FAPI-2

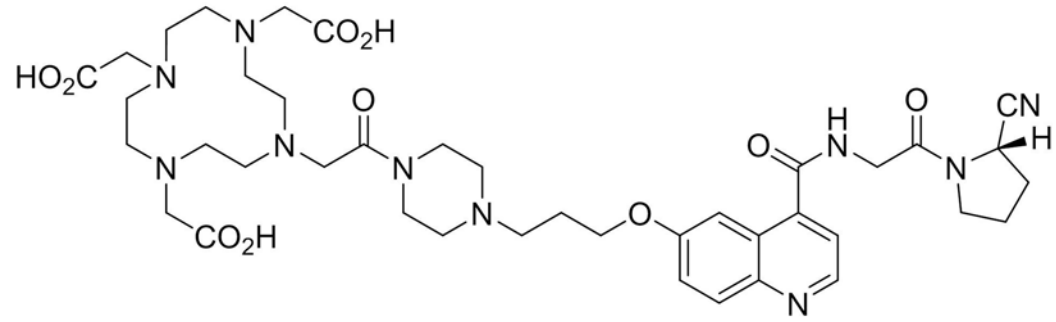

FAPI-4

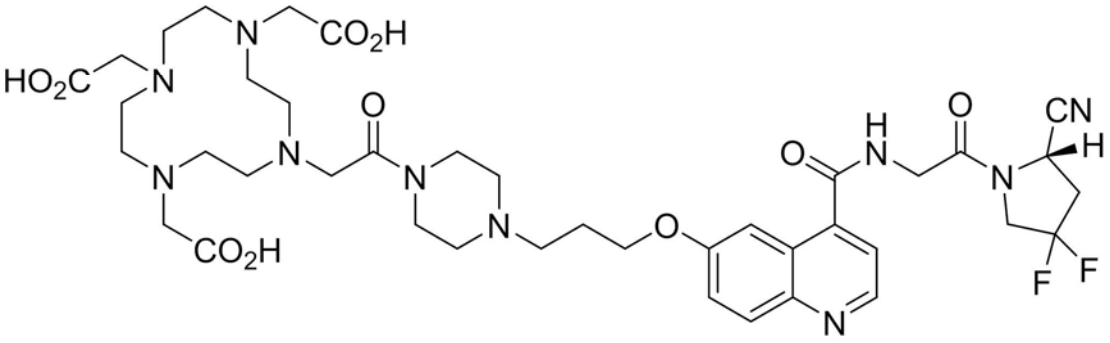

Figure-1: Molecular structure of FAPI-2 and FAPI-4.

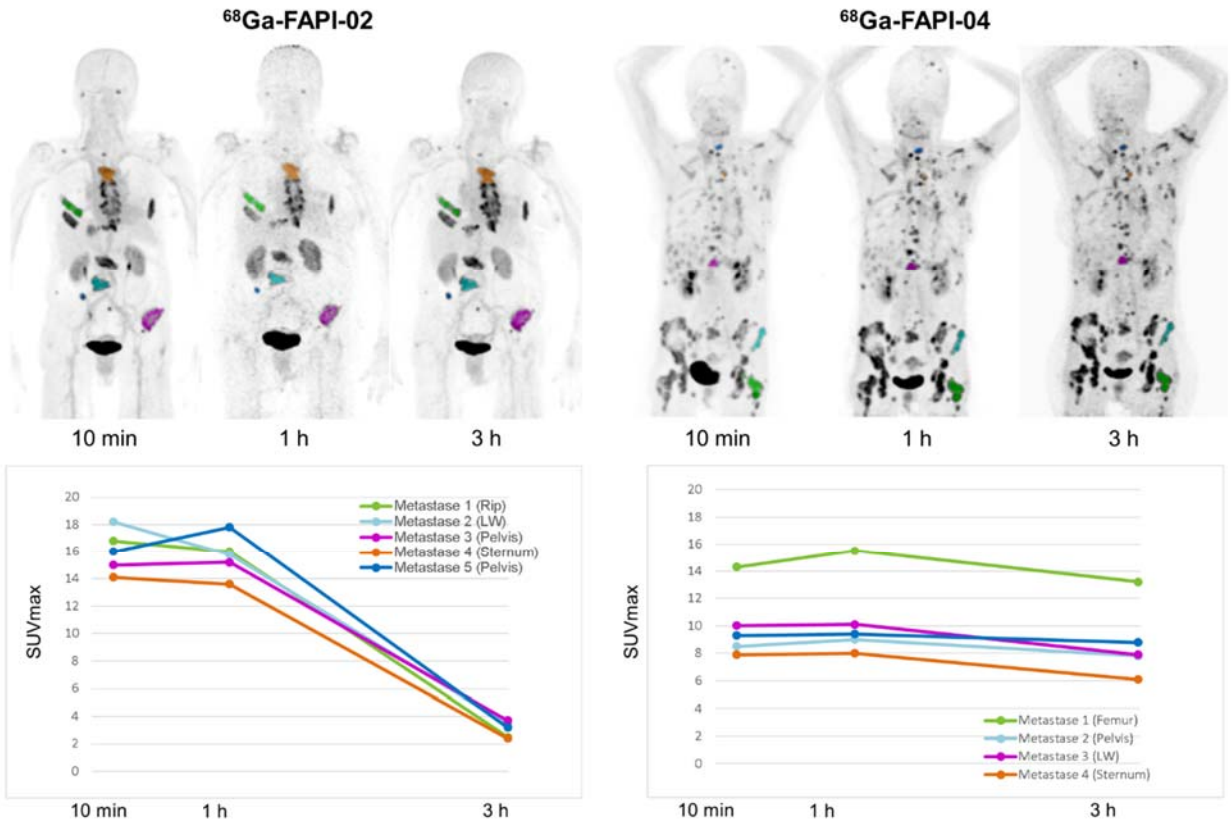

Figure-2: FAPI-2 and FAPI-4 at the different imaging time-point (10 min., 1h and 3h p.i.) in two patients with metastasized breast cancer. Rapid tumor targeting and fast blood clearance is followed by a long plateau phase without relevant change in image contrast (top). In comparison to FAPI-02 the ligand FAPI-04 is characterized by a prolonged tumor retention time (bottom).

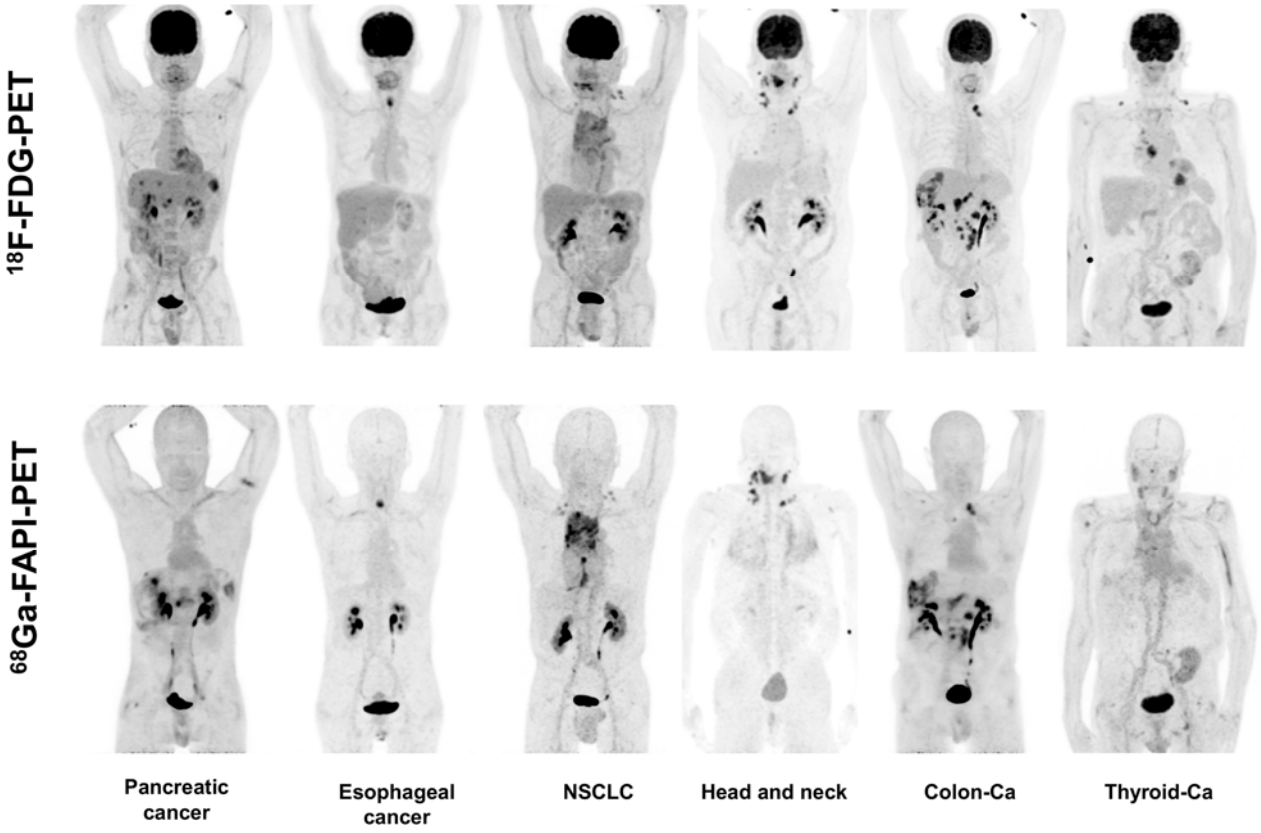

Figure-3: Intra-individual comparison of 6 patients with 6 different tumor entities undergoing FDG-PET and FAPI-PET imaging within <9 days. 5 / 6 patients present similar strong tumor uptake with FDG and FAPI and 3 / 6 could benefit from lower background in liver or pharyngeal mucosa. In contrast, a iodine-negative thyroid cancer patient presented only minor FAPI tracer uptake compared to FDG.

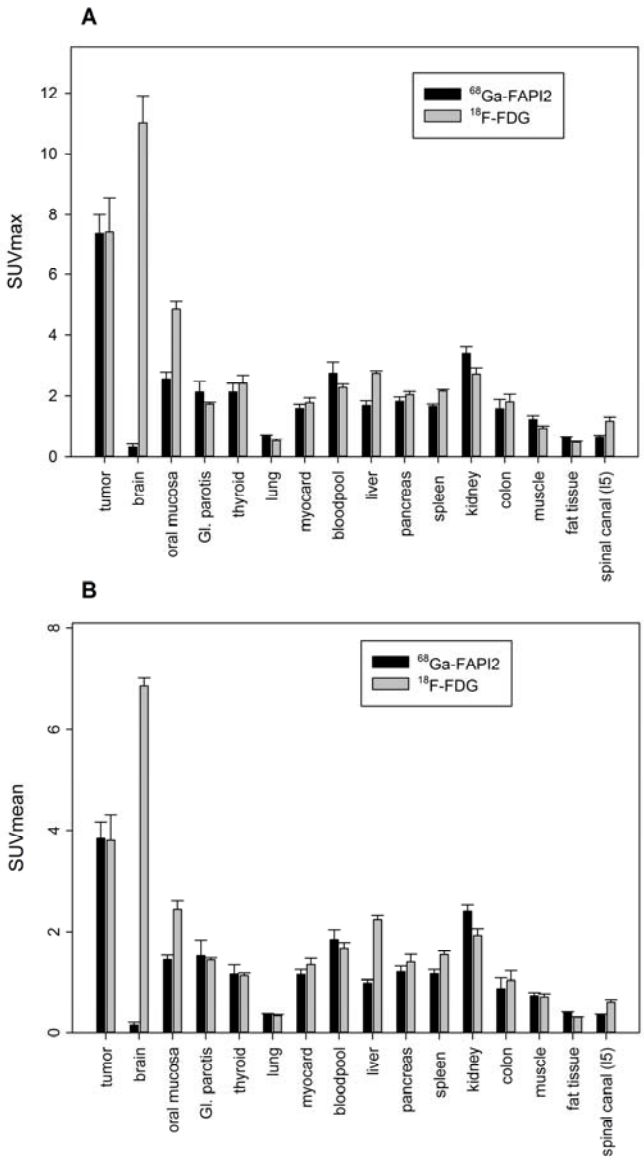

Figure-4:

PET-based biodistribution analysis of the 6 patients intra-individually comparing FDG-PET and FAPI-PET, imaged at 1h p.i., respectively.

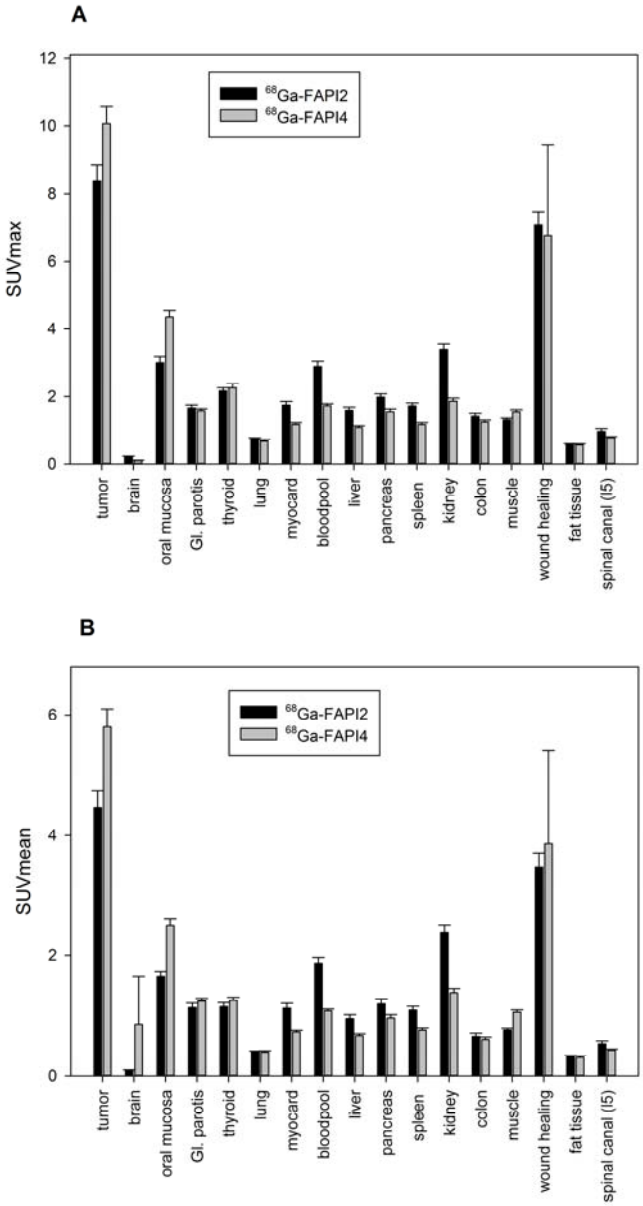

Figure-5:

Inter-individual comparison of 25 patients examined with FAPI-2 and 25 patients examined with FAPI-4 PET at 1h p.i. respectively.

Table-1: Patient characteristics

Patient no.	Gender	Age	MBq	Diagnose	Tracer
1	f	89	312	breast cancer	FAPI-02
2	m	55	298	colorectal cancer	FAPI-02, FDG
3	m	56	256	CUP	FAPI-02
4	m	64	336	head and neck cancer	FAPI-02
5	m	66	196	head and neck cancer	FAPI-02
6	f	64	202	head and neck cancer	FAPI-02
7	f	65	178	head and neck cancer	FAPI-02
8	m	59	325	head and neck cancer	FAPI-02
9	m	68	255	head and neck cancer	FAPI-02, FDG
10	m	70	212	hepatocellular carcinoma	FAPI-02
11	m	66	308	liposarcoma	FAPI-02
12	m	78	222	NSCLC	FAPI-02, FDG
13	f	66	268	NSCLC	FAPI-02
14	f	58	126	oesophagus cancer	FAPI-02, FDG
15	m	70	134	oesophagus cancer	FAPI-02
16	m	31	307	pancreatic cancer	FAPI-02, FDG
17	m	52	167	pancreatic cancer	FAPI-02
18	m	56	222	pancreatic cancer	FAPI-02
19	f	73	142	pancreatic cancer	FAPI-02
20	m	74	122	prostate cancer	FAPI-02
21	m	77	318	prostate cancer	FAPI-02
22	m	60	285	renal cell carcinoma	FAPI-02
23	m	77	225	thyroid cancer	FAPI-02, FDG
24	m	55	270	thyroid cancer	FAPI-02
25	f	60	238	uterus cancer	FAPI-02
26	f	57	263	breast cancer	FAPI-04
27	f	44	220	colorectal cancer	FAPI-04
28	m	66	286	colorectal cancer	FAPI-04
29	m	55	244	colorectal cancer	FAPI-04
30	m	46	247	CUP	FAPI-04
31	f	82	236	head and neck cancer	FAPI-04
32	m	51	263	head and neck cancer	FAPI-04
33	m	84	246	hepatocellular carcinoma	FAPI-04
34	m	77	299	NSCLC	FAPI-04
35	f	58	217	NSCLC	FAPI-04
36	m	64	255	NSCLC	FAPI-04
37	f	56	250	ovarian cancer	FAPI-04
38	f	67	260	pancreatic cancer	FAPI-04
39	f	76	243	pancreatic cancer	FAPI-04
40	f	55	293	pancreatic cancer	FAPI-04
41	m	52	239	pancreatic cancer	FAPI-04
42	m	61	198	pancreatic cancer	FAPI-04
43	m	73	277	pancreatic cancer	FAPI-04
44	m	57	275	pancreatic cancer	FAPI-04
45	m	60	237	pancreatic cancer	FAPI-04
46	m	31	233	pancreatic cancer	FAPI-04
47	m	71	249	prostate cancer	FAPI-04
48	m	64	227	prostate cancer	FAPI-04
49	m	72	276	thyroid cancer	FAPI-04

50	f	27	204	thyroid cancer	FAPI-04

Table-2: Dosimetry estimate (OLINDA)

	FAPI-2	**FAPI-4**
Adrenals	1.23E-02	1.12E-02
Brain	9.54E-03	9.11E-03
Breasts	9.58E-03	8.88E-03
Gallbladder Wall	1.19E-02	1.13E-02
LLI Wall	1.23E-02	1.17E-02
Small Intestine	1.19E-02	1.13E-02
Stomach Wall	1.13E-02	1.06E-02
ULI Wall	1.17E-02	1.11E-02
Heart Wall	4.73E-02	2.02E-02
Kidneys	4.45E-02	4.43E-02
Liver	1.51E-02	1.46E-02
Lungs	1.09E-02	9.89E-03
Muscle	1.04E-02	9.91E-03
Ovaries	1.24E-02	1.19E-02
Pancreas	1.23E-02	1.13E-02
Red Marrow	3.28E-02	2.08E-02
Osteogenic Cells	2.94E-02	2.16E-02
Skin	9.01E-03	8.63E-03
Spleen	2.62E-02	1.05E-02
Testes	1.04E-02	1.01E-02
Thymus	1.15E-02	1.01E-02
Thyroid	1.03E-02	9.82E-03
Urinary Bladder Wall	8.89E-02	9.91E-02
Uterus	1.33E-02	1.30E-02
Total Body	1.19E-02	1.09E-02
Effective Dose (mSv/MBq)	1.80E-02	1.64E-02